Journal of Engineering and Sustainable Development
Vol. 29, No. 06, November 2025
https://jeasd.uomustansiriyah.edu.iq/index.php/jeasd
ISSN 2520-0917
Research Article
https://doi.org/10.31272/jeasd.2565

Simulation of Two-Phase Flow Pollutant Transport in Porous Media Using Experimental and CFD Model

Sadiq S. Muhsun[1]*, Sanaa A. Talab Al-Osmy[1], Faris Hamid[2], Zainab T Al-Sharify[3], Noureddine Elboughdiri[4]

[1]Water Resources Engineering Department, College of Engineering, Mustansiriyah University, Baghdad, Iraq.
[2]Environmental Engineering Department, College of Engineering, Mustansiriyah University, Baghdad, Iraq.
[3]Al Hikma University College, Baghdad, Iraq.
[3]Department of Chemical Engineering, University of Birmingham, Edgbaston B15 2TT, Birmingham, United Kingdom.
[4]Chemical Engineering Department, College of Engineering, University of Ha'il, Ha'il 81441, Saudi Arabia. [4]Chemical Engineering Process Department, National School of Engineers, University of Gabes, Gabes 6029, Tunisia

*Email: sadiq.aljilizy@uomustansiriyah.edu.iq

Article Info

Received	**29/04/2024**
Revised	**31/08/2025**
Accepted	**15/09/2025**

Abstract

In this work, a physical model and a Computational Fluid Dynamics simulation model in COMSOL software version 6.4 were used to simulate the two-stage transport of pollutants through porous Media. As for the physical model, it was manufactured in a laboratory to conduct practical experiments to verify two-phase flow through sandy soil. Kerosene (as a pollutant in this work) was pumped through the porous medium in different experiments at mixing ratios (100%, 85% oil to water), such that this stage represents the pollution stage. At the end of each pollution stage, the soil is washed by pumping clear water to represent the washing process. Based on standard statistical indicators, it was found that the Computational Fluid Dynamics simulation model consistently yields water-saturated ratio S1 and oil-saturated ratio S2 that are close to reality, with an acceptable error rate. This indicates the ability of Computational Fluid Dynamics models to simulate the complex two-stage pollutant transport process through porous media with high accuracy and in a short time, at lower cost and effort.

Keywords: Computational fluid dynamics, COMSOL, Physical model, Porous media, Seepage physical model, Soil pollution.

1. Introduction

Understanding the dynamics of multiphase flow in porous media presents intriguing challenges for authors and engineers across a range of disciplines. The investigation of how multiphase flow behaves within porous media is of paramount importance across a range of sectors, including nuclear waste containment, improved oil recovery, groundwater purification, and geological sequestration of carbon dioxide. Understanding the nature of multiphase flow is also important for understanding particle flow in vascular bifurcations or classifying fluid transport through cellulose [1], [2]. Multiphase flow refers to the movement of substances in multiple states of aggregation. These states can encompass solids, liquids, or gases in a continuous or distinct phase. In simulation contexts, a phase is a distinct quantity of matter within a system, possessing unique physical characteristics that differentiate it from other phases [3], [4].

Two-phase flow is a specific case within the broader category of multiphase flow, involving solely two distinct constituents. These two phases can encompass gas-solid flow (as in fluidized beds), liquid-solid flow (as in slurry flow), or liquid-gas flow (as in boiling and condensation processes). Additionally, mixtures may involve liquid-liquid or gas-gas interactions, and in more comprehensive situations, there may exist more than two phases. The configuration of two-phase streams is notably varied, contingent on the size and dispersion of the phase elements within a continuous medium, as well as their direct interactions. Examples of naturally occurring two-phase media include smoke, smog, haze, and rain, while in engineering and technology, instances like emulsions, sludge, and boiling liquids are common [5], [6]. The importance of numerically simulating two-phase flows is highlighted by the fact that, historically, the most common method for working with such materials has been experimental. The definition of pressure, phase, and other relevant parameters in two-phase flows has been simplified by contemporary advances in computational

hardware and numerical techniques. For a multitude of engineering applications, these insights are invaluable [7].

The initial modeling of the flow of two fluids within a soil structure can be reduced to a two-phase flow within porous media. This leads to extensive work into their complex dynamics through various computational approaches, including computational fluid dynamics (CFD) techniques. As a subset of fluid mechanics, CFD uses numerical methods to address and investigate fluid dynamics problems, many of which are expensive or even impossible in real experiments [8]. Numerical simulation has been used for many years to address practical issues across many aspects of our lives. Simulations can help you understand physical phenomena across a wide range of industrial and non-industrial fields when combined with experiments. As computational fluid dynamics (CFD) has been integrated into academic and manufacturing fields, it has emerged as a valuable and promising tool capable of accurately predicting many complex phenomena, even in highly complex systems.

The main advantages of CFD are the ability to explore multiple parameters within the same problem without incurring significant additional overhead, the ability to perform comprehensive works of the simulated phenomenon by measuring variables that may not be precisely determined by experimental means, and the lower cost compared to experiments, and such are just a few of the important advantages offered by CFD [9]. Computational fluid dynamics (CFD) has been demonstrated to be effective for modeling particle motion in indoor environments. CFD enables the creation of realistic, cost-effective, large-scale simulations and the visualization of transport processes, and facilitates an in-depth understanding of complex physical phenomena [10]. COMSOL Multiphysics is a simulation program that includes all the necessary steps for modeling a workflow. This process involves specifying the geometries, material properties, and physics that define the phenomena being modeled, and using these specifications to generate modeling solutions and post-process them to produce accurate, trustworthy results. COMSOL can be used to model a combination of physics for a given unit phenomenon, enabling engineers or scientists to apply it to a specific field application. It can also import designs from other computer programs using interface products that make it easy to recognize geometric shapes and export the results to others [11].

In this work, practical and numerical studies were conducted on two-phase pollutant transport in porous media, particularly sandy soil, using the COMSOL simulation program to describe and explain this phenomenon, which remains underexplored and warrants further investigation, considering COMSOL ver. 6.4 to analyze and describe this complicated issue to provide the required results may be the first try, as was seen in a wide range of works.

2. Method of the Research

2.1. Model Design

The model consists of two acrylic polymer pipes, each 4 m long, 0.08 m in diameter, and 0.005 m thick. In general, each pipe is designated for a specific type of soil: the first for sandy soil and the second for organic soil. For brevity, this paper focuses on the first media only (sandy soil), with the remaining results for the second soil presented and compared in a subsequent work. However, in every half meter of the length of the pipe, there is an opening with a diameter of 0.01 meters. It is connected to a small tube, 0.03 m long, for collecting samples and measuring pressure with a manometer. Filters are placed in each hole to prevent soil from escaping. Seven points were placed on each pipe to collect samples during operation over time and along the length of the pipe. Unfortunately, due to labor issues with operating the system and sampling, part of the pipe was destroyed during the experiments, reducing its length from 4 m to 3 m.

Therefore, the number of points decreased from 7 to 5 in recent work experiments. The pipes are placed on a horizontal iron stand at a height of 1.5 meters above the ground. This is to make the flow identical to the real groundwater flow, which is always assumed to be horizontal and to have horizontal streamlines [12]-[14]. However, at the end of the pipes, there is a tank with a capacity of 0.25 m^3 for pumping water. There is also another tank with a capacity of 0.09 m^3 for oil pumping, along with a pump for transporting oil and water. The pump is connected to valves to control the flow, and these valves are connected to the two pipes through small connectors. A second tank with a capacity of 0.25 m^3 was also placed at the end of the two pipes to collect the final effluent discharge from the pipes, which contains oil and water together.

Fig. 1 shows the general layout of the physical model, while Fig. 2 shows the actual physical model.

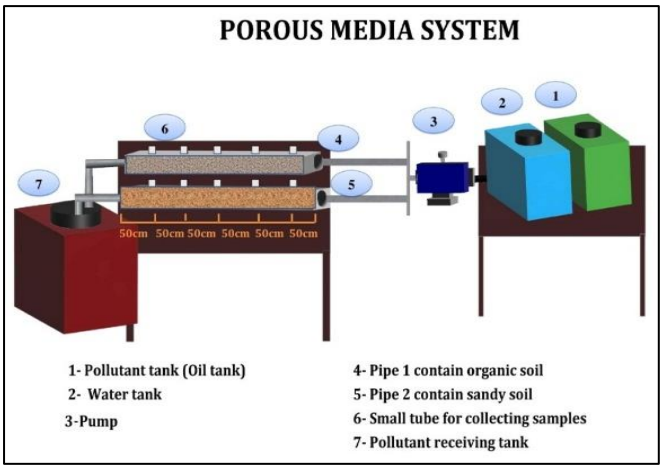

Figure 1. General layout of the physical model.

Figure 2. Laboratory physical model.

2.2. Porous Media

In this work, two types of porous media with different physical properties were used: one was loose and incoherent. The other was more cohesive, aimed at determining the effect of this difference on the behavior of pollutant flow in two phases, but due to the large number of results and the magnitude of the work. The focus in this work is only on the first type, which involves sifted sandy soil to remove large pebbles and impurities. Fig. 3 shows the kind of porous material used. The main physical properties of the used soil, including sieve analysis, porosity, permeability, and bulk density, are presented in Table 1.

Figure 3. Sandy soil was used as media.

Table 1. Laboratory results of the porous media used.

Soil	Permeability (m/s)	Porosity	Bulk density (g/cm^3)
Sandy	2.07E-05	0.35	1.59

2.3. Pollutant

In this work, approximately 0.2 m^3 of kerosene was used as the contaminant, along with a second fluid, water. Kerosene is a commonly used substance in daily life and readily permeates soil. It demonstrated no pore-clogging or complications in the laboratory model, primarily because it falls under the category of light oils and its density (0.81 $g.cm^{-3}$). The classification of oils into light and heavy categories is determined based on their density. Density is quantified following the specific density scale as per the American Petroleum Institute standards, and a mathematical formula exists for specific density calculation. As mentioned previously, oil is categorized as heavy (0.91 to 1.05 g/cm^3), medium (0.87 - 0.91 g/cm^3), and light (0.65 to 0.87 g/cm^3) when the API density is less than 22.30 [15].

2.4. Experimental Work with Physical Model

Two different types of experiments were conducted depending on the percentage of saturated water ratio S1 or saturated oil ratio S2 flowing through the porous medium, as follows:

2.4.1. First type experiment (100% oil ratio, S1=0 and S2 = 1)

This experiment begins by turning on the water pump and allowing the soil to moisten for 1 to 2 hours. Only then does oil start pumping; i.e., 100% oil (S1 = 0 and S2 = 1) is allowed to flow into the pipes. In general, after half an hour, the first groups of samples were drawn from the sampling points distributed along the pipe instantaneously. Half an hour later, the second group of samples was also drawn, and the sampling continued at each time point until the S2 ratio reached 100%. In other words, the physical model continues to run until the oil percentage (S2) reaches 100% at the endpoint, which is the contamination stage. After that, oil pumping stopped, and water pumping resumed, marking the soil-washing stage. The washing stage continues for a period depending on the type of soil and the flow rate. During this stage, samples were also drawn as described above to measure the decrease in the saturated oil ratio (S2) or the increase in the water saturation ratio (S1) at each point. In both stages (contamination or washing), the collected samples from the designated points (7 or 5 points) were placed in a graduated cylinder to estimate the saturated water (S1) and saturated oil (S2) ratios. However, S1 and S2 should always be equal to 100%.

2.4.2. Second type experiment (S1 ≠0 & S2 ≠1)

In this experiment, the same practical steps were followed as in the first experiment, except for the pollution pumping stage. This time, the oil was not pumped with S2=100%, but was mixed with a certain percentage of water and injected into the soil simultaneously. A mixing tank was designed to mix oil and water throughout the process of pumping pollutants, and several mixing ratios were evaluated; the optimal ratio was approximately 15% water to 85% oil (S1 = 15% and S2 = 85%). Fig. 4 shows the designed mixing tank used in the second experiment. However, the proportions of the mixture were

measured even after it entered the soil to ensure they remained the same when it entered the porous medium.

Figure 1. Mixing tank of the second experiment.

Samples were collected at different time points, as in the first experiment, to determine the oil-to-water volume ratio (S1 and S2). The physical model continues to run until the oil percentage (S2) reaches 85% at the end point of the first pipe of the contamination stage. Then the soil washing process (Washing stage) was carried out, and samples were collected again at different intervals to evaluate the percentage of remaining oil (S2) after washing. The saturated percentage of water and oil (S1 and S2) in each sample from both experiments was estimated using (1), (2), and (3):

$$S1 = \frac{volume\ of\ water}{total\ volume\ (oil + water)}\ 100\% \quad (1)$$

$$S2 = \frac{volume\ of\ oil}{total\ volume\ (oil + water)}\ 100\% \quad (2)$$

$$\text{Or} \quad S1 + S2 = 100 \quad (3)$$

Where S1 and S2 are the water and oil saturated ratios (fractions), respectively.

2.5. CFD Simulation Model

To align with the dimensions utilized in the laboratory-based physical model, a 2D symmetric CFD model was developed. The physics considered in this CFD model is Two-Phase Darcy's Law (TPDL), which is used to simulate fluid flow through the voids of a porous medium. It solves Darcy's law for the overall pressure and tracks the transport of fluid content within a single fluid phase. The physics interface can be used to model situations with slow flows (in a medium with low permeability) and a porous structure. The pressure gradient is the primary force at work here, with the frictional resistance within the porous structure playing a significant role in shaping the flow dynamics [16].

2.5.1. Govern equations

The following system of differential equations represents the (4, 5, 6, 7, 8, 9, and 10) equations that govern the phenomenon [17], [18].

$$\frac{\partial n\rho}{\partial t} + \nabla.(\rho u) = 0 \quad (4)$$

$$u = -\frac{k}{\mu}\Delta p2 \quad (5)$$

$$\rho = S_1\rho_1 + S_2\rho_2 \quad (6)$$

$$\frac{1}{\mu} = S_1\frac{kr_1}{\mu_1} + S_2\frac{kr_2}{\mu_2} \quad (7)$$

$$S_1 + S_2 = 1 \quad (8)$$

$$\frac{\partial nc1}{\partial t} + \nabla.(c1u) = \nabla.(D_c\nabla c1) \quad (9)$$

$$c_1 = S_1\rho_1 \quad (10)$$

Where: ρ = fluid density (kg/m^3)

N = porosity (fraction)

p = pressure in Pa

Kr = relative permeability

u = Velocity field in x- direction, m/s

$\mu = Dynamic\ viscosity\ in\ Pa.s$

Other variables are as previously defined.

2.5.2. Initial and boundary conditions

Boundary conditions were verified through velocity and pressure conditions such that:

Boundary Conditions B.C.

For entry at x = 0, V = Vin, inlet velocity

For the outlet at x = L, P = Po = Zero

The boundary condition of the saturated water ratio S1 at the inlet is considered as follows,

For the pollutant stage

S1 = 0 or 0.15 at x = 0, (inlet point)

Corresponding to 100% or 85% of the saturated oil ratio, respectively.

For the washing stage

S1 = always 1 at x = 0, (inlet point)

Initial condition I.C.

at t = 0, everywhere for p(x,y) the following conditions are verified. For the saturated water-to-oil ratios S1 & S2, the pollutant stage uses S1 = 1, while the washing stage uses S1 = 0 or 0.15, corresponding to 100% or 85% of S2, respectively. For more explanations, see Fig.5.

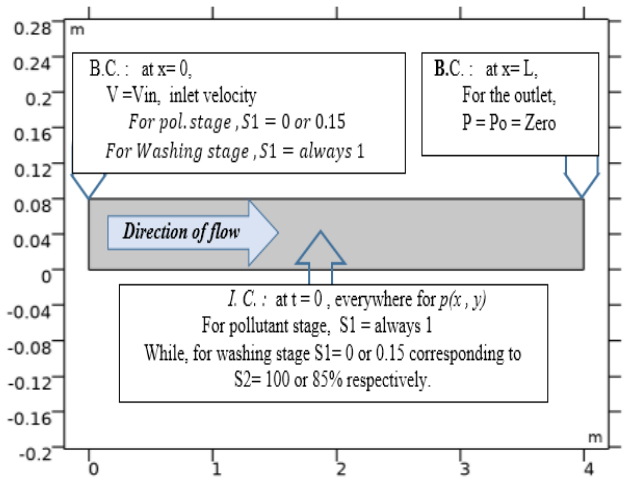

Figure 2. Boundary and initial conditions of the CFD simulated model.

2.5.3. Mesh design

According to the length of the pipe, the design mesh used in CFD model is an excellent triangular element size, with a count between (2006 or 1506) elements, (4 or 4) vertexes elements and (408 or 308) edges elements as shown in Fig. 6. The adoption of this design for the mesh was considered after some operational attempts of the program with various meshes to reach the optimal mesh dimensions that do not affect the accuracy of the results and do not take up a lot of time or memory.

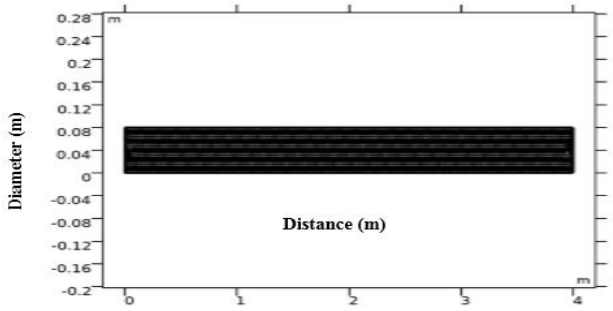

Figure 3. Design a mesh for a 4m pipe length.

3. Results and Discussion

3.1. Results of the Physical Model and CFD Simulated Model

3.1.1. Pollutant and washing states 100% oil ratio

Fig. 7(a)-7(d) shows the results for the water-saturated ratio S1 and the oil-saturated ratio S2 during the pollution and washing stages, respectively. By comparing the results from the physical and CFD models, it is clear that the CFD model produces results that are very impressive and acceptable. They note the strong agreement between their results and those of the physical model, indicating the strength of the CFD-simulated model, which was created to simulate and predict the spread of oil through porous media. The results were obtained due to the operation of the physical model and the CFD simulated model with an oil flow rate of 100% (S1=0, S2=100%) and a discharge of 0.0664 l/min or a velocity of 0.00022 m/s for the pollution stage and with a flow rate of 100% water (S1=100% & S2=0%) and a discharge of 0.0392 l/min or a velocity of 0.00013 m/s for the washing stage.

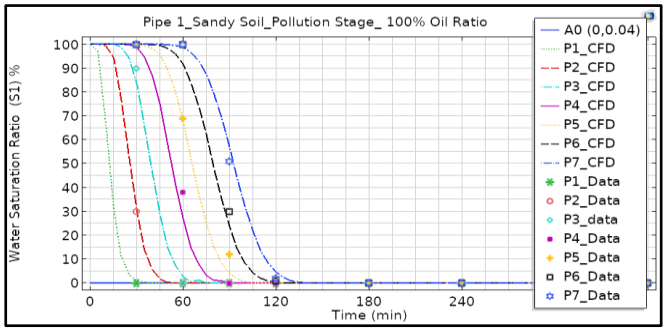

Figure 4 (a). Physical and CFD results for the water-saturated ratio (S1) for the 100% oil ratio, pollution stage.

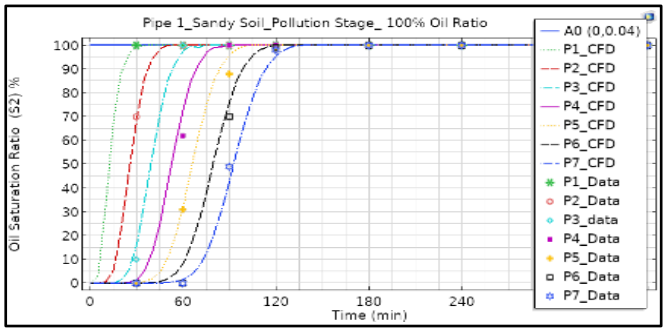

Figure 7 (b). Physical and CFD results for the oil-saturated ratio (S2) for the 100% oil ratio, pollution stage.

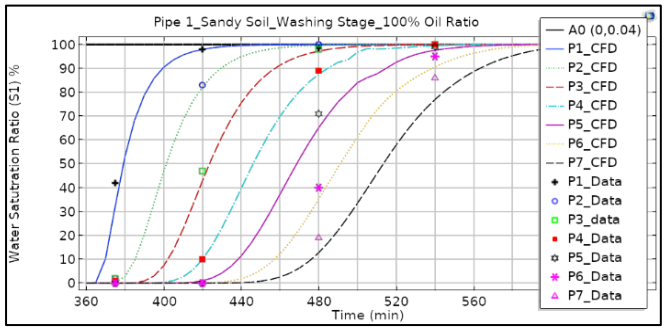

Figure 7 (c). Physical and CFD results for the water-saturated ratio (S1) for the 100% oil ratio, washing stage.

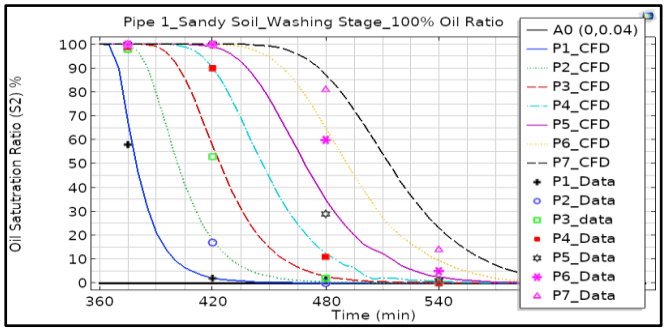

Figure 7 (d). Physical and CFD results for the oil-saturated ratio (S2) for a 100% oil ratio in the washing stage.

3.1.2. Pollutant and washing staged 85% oil ratio

Fig. 8(a)-8(d) shows all the CFD results and their comparison with the experimental results for the 85% oil ratio case. However, in this experiment, for the pollutant stage, the S2 at each checkpoint increases from 0 to 85%. In comparison, the ratio of saturated water S1 decreases from 1 to 15%, maintaining the stability condition in the two-face flow, so that (S1 + S2 = 100) is satisfied at all points and times. So, after ensuring that the oil-saturated ratio S2 at the last point reached 0.85 (i.e., S1 = 15%), oil pumping was stopped, and the pollution stage was over. The results also indicate a very good agreement between the physical and CFD models.

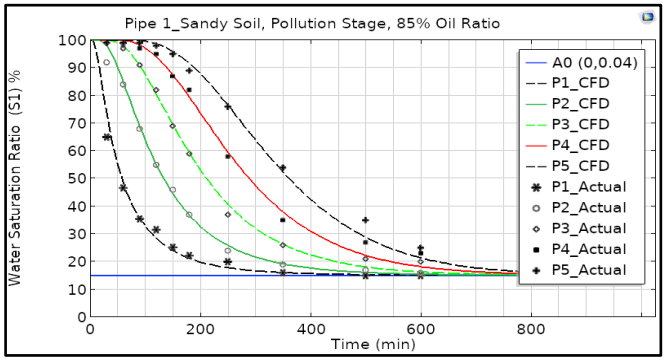

Figure 8 (a). Physical and CFD results for the water-saturated ratio (S1) for the 85% oil ratio, pollution stage.

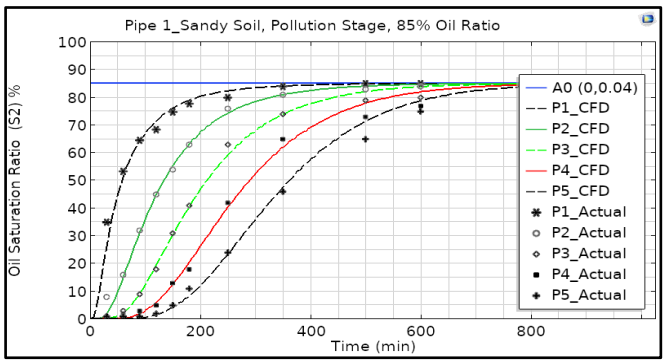

Figure 8 (b). Physical and CFD results for the oil-saturated ratio (S2) for the 85% oil ratio, pollution stage.

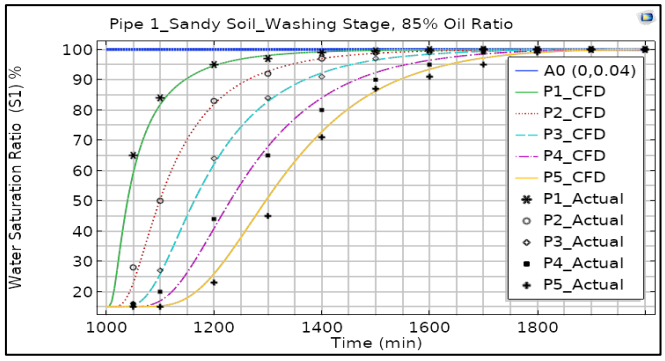

Figure 8 (c). Physical and CFD results for the water-saturation ratio (S1) for an 85% oil ratio during the washing stage.

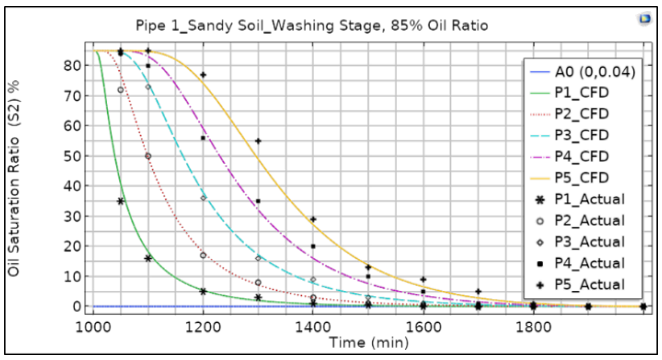

Figure 8 (d). Physical and CFD results for the oil saturated ratio_S2 in the case of an 85% oil ratio, washing stage.

3.2. Statistical Verification

In this part, the results of the CFD program and the actual results were verified using the standard statistical indicators shown in (11), (12), (13), and (14), as well as in Tables 2 to 5 [19], [20]**.** Based on these statistical indicators, the simulation model provides expected results that closely match reality. This means that CFD-simulated models can be relied upon as a tool to solve many cases of such complex problems without the need for a physical model, thus reducing time, effort, and cost.

$$\mathrm{RMSE} = \left[\left(\frac{1}{n}\sum_{i=1}^{n}(S_m - S_s)^2\right)\right]^{1/2} \quad (11)$$

$$\mathrm{MSE} = \frac{1}{n}\sum_{i=1}^{n}(S_m - S_s)^2 \quad (12)$$

$$\mathrm{MAE} = \frac{1}{n}\sum_{i=1}^{n}|S_m - S_s| \quad (13)$$

$$\mathrm{RSE} = \frac{\sum_{i=1}^{n}(S_m - S_s)^2}{\sum_{i=1}^{n}(S_m - \overline{S_m})^2} \quad (14)$$

Where:

RMSE: root mean squared error,

MSE: mean squared error,

MAE: mean absolute error.

RSE: relative squared error

n: total observed data

$\overline{S_m}$: The mean of S_Ratio measured,

S_m: S $_{\text{measured}}$

S_s: S $_{\text{Simulated}}$

Table 2. S2_Statistical analysis verifications of 100% oil ratio, pollutant stage.

Points	RMSE	MSE	MAE	RSE
P1	0.0998	0.0100	0.0650	0.0813
P2	0.0644	0.0041	0.0243	0.0000
P3	2.5138	6.3193	0.9501	0.0064
P4	4.4133	19.4769	1.6681	0.0161
P5	3.1813	10.1209	1.6533	0.0068
P6	2.6077	6.8003	1.1065	0.0036
P7	2.2437	5.0340	1.1150	0.0023

Table 3. S2_Statistical analysis verifications of 100% oil ratio, washing stage.

Points	RMSE	MSE	MAE	RSE
P1	3.7696	14.2102	1.6272	0.0351
P2	0.6997	0.4895	0.3540	0.0004
P3	1.8007	3.2424	1.0122	0.0025
P4	0.7523	0.5659	0.4073	0.0003
P5	2.2003	4.8412	1.1024	0.0025
P6	2.1981	4.8315	1.1720	0.0024
P7	2.6700	7.1289	1.4085	0.0032

Table 4. S2_Statistical analysis verifications of 85% Oil ratio, pollutant stage.

Points	RMSE	MSE	MAE	RSE
P1	2.7897	7.7825	1.6221	0.0337
P2	1.9361	3.7484	1.1379	0.0051
P3	1.9383	3.7571	1.3665	0.0037
P4	2.5647	6.5777	2.0635	0.0062
P5	2.4680	6.0912	1.8014	0.0059

Table 5. S2_Statistical analysis verifications of 85% oil ratio, washing stage.

Points	RMSE	MSE	MAE	RSE
P1	1.9123	3.6571	0.8982	0.0340
P2	1.6062	2.5799	0.7299	0.0048
P3	0.9007	0.8113	0.6488	0.0009
P4	2.1832	4.7665	1.6697	0.0049
P5	2.3219	5.3914	1.4872	0.0045

4. Conclusions

The results above show that, in terms of values, the spread of pollutants and the exchange ratios between S1 and S2 are faster in sandy soils, both during the pollution stage and the washing stage. The concentration of the pollutant S2 in the porous medium is directly proportional to the entry speed. As the spread speed increases with the entry speed, so does the concentration, whether in the pollution or washing stage. Pollution rates in the porous medium S2 are strongly affected by the mixing ratio of the Pollutant with the water entering the medium, regardless of whether it is 100% or less. The distributions of water S1 and pollutant S2 change nonlinearly with distance and time, but remain constant in the direction perpendicular to the flow and change only with time. Based on several statistical indicators, the CFD simulation model agrees very well with the corresponding experimental results of the physical model across all tested cases, without requiring the creation of a physical model that would increase effort, time, and costs.

In upcoming work, the results of the physical model and the CFD dynamic model for two-phase flow in organic soils will be presented and compared with those in sandy soils. Also, a separate work will examine the effects of the most important physical factors of soil — such as porosity, permeability, and density — as well as the hydraulic characteristics of flow — such as velocity and viscosity — on the flow of two-phase pollutants in porous media.

Acknowledgements

The authors would like to thank Mustansiriyah University (www.uomustansiriyah.edu.iq), Baghdad, Iraq, for their support in the present work. Also, thanks to the staff of the Hydrology, Hydraulics, Sanitary, and Soil Laboratories at the College of Engineering for their efforts and assistance throughout the work. The authors also thank the National Centre for Construction Laboratories Department of Soil Investigation for conducting some tests.

Conflict of interest

The author declares that there are no conflicts of interest regarding the publication of this manuscript.

Author Contribution Statement

Sadiq S. Muhsun prepared the laboratory model and CDF model.

Sanaa A. Talab Al-Osmy collected data and analyzed the results.

Faris Hamid collected data, prepared figures, and collected references.

Zainab T. Al-Sharify collected data, collected references, Noureddine Elboughdiri audited the results, and participated in preparing the CFD model.

References

[1] A. L. Herring, E. J. Harper, L. Andersson, A. Sheppard, B. K. Bay, and D. Wildenschild, "Effect of Fluid Topology on Residual Nonwetting Phase Trapping: Implications for Geologic CO2 Sequestration," Advances in Water Resources, vol. 62, pp. 47–58, Dec. 2013, doi: https://doi.org/10.1016/j.advwatres.2013.09.015.

[2] H. Wang et al., "Modeling of multi-scale Transport Phenomena in Shale Gas Production — a Critical Review," *Applied Energy,* vol. 262, p. 114575, Mar. 2020, doi: https://doi.org/10.1016/j.apenergy.2020.114575.

[3] D. Gläser, B. Flemisch, R. Helmig, and H. Class, "A hybrid-dimensional Discrete Fracture Model for non-isothermal two-phase Flow in Fractured Porous Media," *GEM - International Journal on Geomathematics*, vol. 10, no. 1, Jan. 2019, doi: https://doi.org/10.1007/s13137-019-0116-8.

[4] A. Mikelić, M. F. Wheeler, and T. Wick, "Phase-field Modeling through Iterative Splitting of Hydraulic Fractures in a Poroelastic Medium," Gem - *International Journal on Geomathematics*, vol. 10, no. 1, Jan. 2019, doi: https://doi.org/10.1007/s13137-019-0113-y.

[5] T. Feng et al., "Numerical Research on Thermal Mixing Characteristics in a 45-degree T-junction for two-phase Stratified Flow during the Emergency Core Cooling Safety Injection," *Progress in Nuclear Energy*, vol. 114, pp. 91–104, Jul. 2019, doi: https://doi.org/10.1016/j.pnucene.2019.03.009.

[6] J. A. Pinilla, E. T. Guerrero, H. Pineda, R. R. Posada, E. Pereyra, and N. Ratkovich, "CFD Modeling and Validation for two-phase Medium Viscosity oil-air Flow in Horizontal Pipes," *Chemical Engineering Communications*, vol. 206, no. 5, pp. 654–671, Sep. 2018, doi: https://doi.org/10.1080/00986445.2018.1516646.

[7] Ryan Anugrah Putra, T. Schäfer, M. Neumann, and D. Lucas, "CFD Studies on the gas-liquid Flow in the Swirl Generating Device," *Nuclear*

Engineering and Design, vol. 332, pp. 213–225, Jun. 2018, doi: https://doi.org/10.1016/j.nucengdes.2018.03.034.

[8] M. GOMEZ-GESTEIRA, "State-of-the-art of Classical SPH for free-surface Flows," *Journal of Hydraulic Research*, vol. 48, no. Extra, p. 0, 2009, doi: https://doi.org/10.3826/jhr.2010.0012.

[9] I. C. Tolias et al., "Best practice guidelines in numerical simulations and CFD benchmarking for hydrogen safety applications," *International Journal of Hydrogen Energy*, vol. 44, no. 17, pp. 9050–9062, Apr. 2019, doi: https://doi.org/10.1016/j.ijhydene.2018.06.005.

[10] Y. Yan, X. Li, and K. Ito, "Numerical Investigation of Indoor Particulate Contaminant Transport Using the Eulerian-Eulerian and Eulerian-Lagrangian Two-Phase Flow Models," *Experimental and Computational Multiphase Flow*, vol. 2, May 2019, doi: https://doi.org/10.1007/s42757-019-0016-z.

[11] COMSOL, "RF Module User's Guide," 2018. Accessed: Aug. 30, 2025. [Online]. Available: https://doc.comsol.com/5.4/doc/com.comsol.help.rf/RFModuleUsersGuide.pdf

[12] A. Bagchi, Groundwater Hydrology by D.K.Todd. John Wiley & Sons, 1980. Accessed: Nov. 21, 2022. [Online]. Available: https://www.academia.edu/1374102/Groundwater_Hydrology_by_D_K_Todd

[13] Zekâi Şen, "Applied Hydrogeology for Scientists and Engineers," *Choice Reviews Online*, vol. 33, no. 06, pp. 33–34, Feb. 1996, doi: https://doi.org/10.5860/choice.33-3334.

[14] P. B. S. Sarma, "Groundwater Development and Management." Springer Nature, 2019. doi: https://doi.org/10.1007/978-3-319-75115-3.

[15] Y. Nakayama, Introduction to Fluid Mechanics. San Diego: Elsevier Science, 2018.

[16] J. Chen, J. W. Hopmans, and M. E. Grismer, "Parameter Estimation of two-fluid Capillary Pressure–saturation and Permeability Functions," *Advances in Water Resources,* vol. 22, no. 5, pp. 479–493, Jan. 1999, doi: https://doi.org/10.1016/s0309-1708(98)00025-6.

[17] Zou Changjun, Y. Yong, and Liu Xiuwen, "Oil Spill Simulation Based on Multiphase Theory," *2020 7th International Conference on Information, Cybernetics, and Computational Social Systems (ICCSS*), pp. 439–443, Jul. 2017, doi: https://doi.org/10.1109/iccss.2017.8091455.

[18] G. N. Ezeh, J. C. Agunwamba, C. N. Ezugwu, and K. C. Onyelowe, "Modelling Crude Oil Spread in Aquatic Environment," *Agh.edu.pl,* 2019. https://badap.agh.edu.pl/publikacja/125728 (accessed Aug. 30, 2025).

[19] S. S. Muhsun, S. A. Talab Al-Osmy, A. Muttaled, and Z. T. Al-Sharify, "Theoretical, CFD Simulation and Experimental Study to Predict the Flowrate across a Square Edge Broad Crested Weir Depending on the End Depth as a Control Section," *Lecture Notes In Civil Engineering*, pp. 15–34, Nov. 2019, doi: https://doi.org/10.1007/978-3-030-32816-0_2.

[20] S. S. Muhsun and A. Sharify, "CFD Simulated Model and Experimental Tests for Critical Depth and Flowrate Estimation over a broad-crested Weir under the Longitudinal Slope Effect," *International Journal of Environment and Waste Management*, vol. 28, no. 1, pp. 41–41, Jan. 2021, doi: https://doi.org/10.1504/ijewm.2021.117006.